

## Expanded View Figures

### Figure EV1. AIB1 interacts with YAP and TEAD in normal mammary epithelial and breast cancer cell lines.

- A AIB1 interacts with YAP/TAZ and TEAD proteins, as part of a larger complex in normal mammary epithelial (MCF10A) and DCIS (MCFDCIS) cells. Co-immunoprecipitations performed with antibodies as indicated in lanes. Immunoblots show co-IP and input lysate; membranes were probed with antibodies as indicated.
- B Western blot analysis of myc-tagged YAP or YAP S94A levels after AIB1 knockdown in the MCF10A cell lines shown in Fig 1A–C.
- C Validation of AIB1 knockdown in the different MCF10A cell lines shown in Fig 1A–C, assessed by RT–qPCR.
- D TEAD motifs are significantly enriched upstream of the *de novo* YAP signature genes in MCF10A cells. HOMER *de novo* motif analysis in promoters and proximal enhancers (–5,000 to +500 of TSS; Hg38) of genes described in Fig 1A–C.
- E Transfection of indicated proteins (Fig 1D) in HEK293T does not increase endogenous expression of additional AIB1, YAP, or TAZ. Western blot analysis of reporter assay lysate expressing ectopically expressed proteins.
- F AIB1 controls endogenous TEAD target levels in MCF10A and MCFDCIS cells. Levels of endogenous TEAD targets were assessed by RT–qPCR.
- G AIB1 is recruited to promoters of TEAD target genes. Chromatin immunoprecipitation (ChIP) performed with indicated antibodies in MCF10A and MCFDCIS cells. Levels of precipitated chromatin assessed by qPCR.
- H AIB1 is required for lysophosphatidic acid (LPA)-induced YAP activation. Levels of endogenous TEAD targets were assessed by RT–qPCR following 1  $\mu$ M LPA treatment for 1 h.
- I AIB1 is increasingly recruited to promoters of TEAD target genes following LPA induction of YAP activity. ChIP performed with indicated antibodies in MCFDCIS cells following 1  $\mu$ M LPA treatment for 1 h.

Data information: Student's *t*-test was used for the statistical analysis in panels (C, F, G, H, and I); data represent the mean  $\pm$  SD from at least three biological replicates (\**P* < 0.05, \*\**P* < 0.01, \*\*\**P* < 0.001, \*\*\*\**P* < 0.0001, ns = not significant). Source data are available online for this figure.

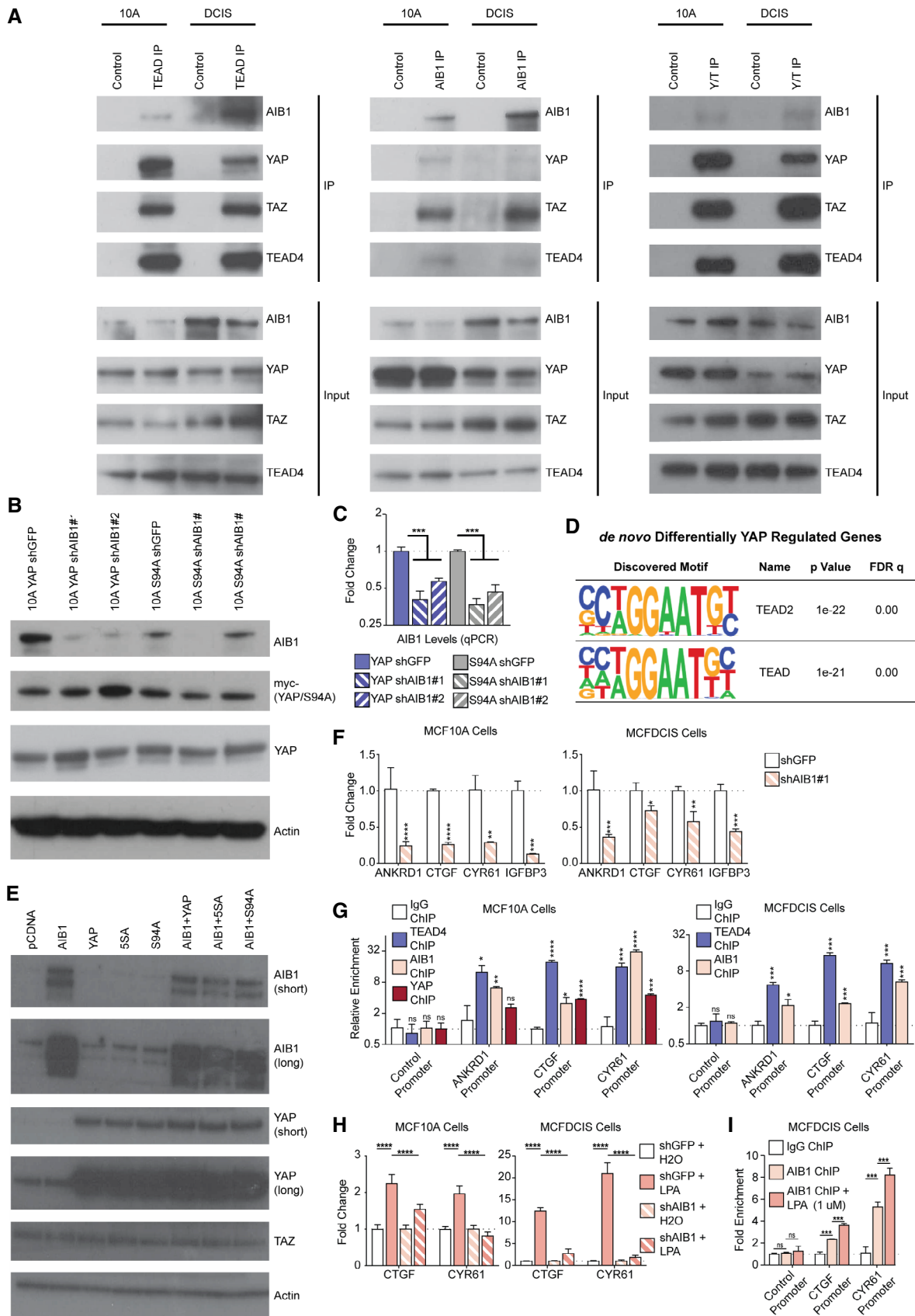


Figure EV1.

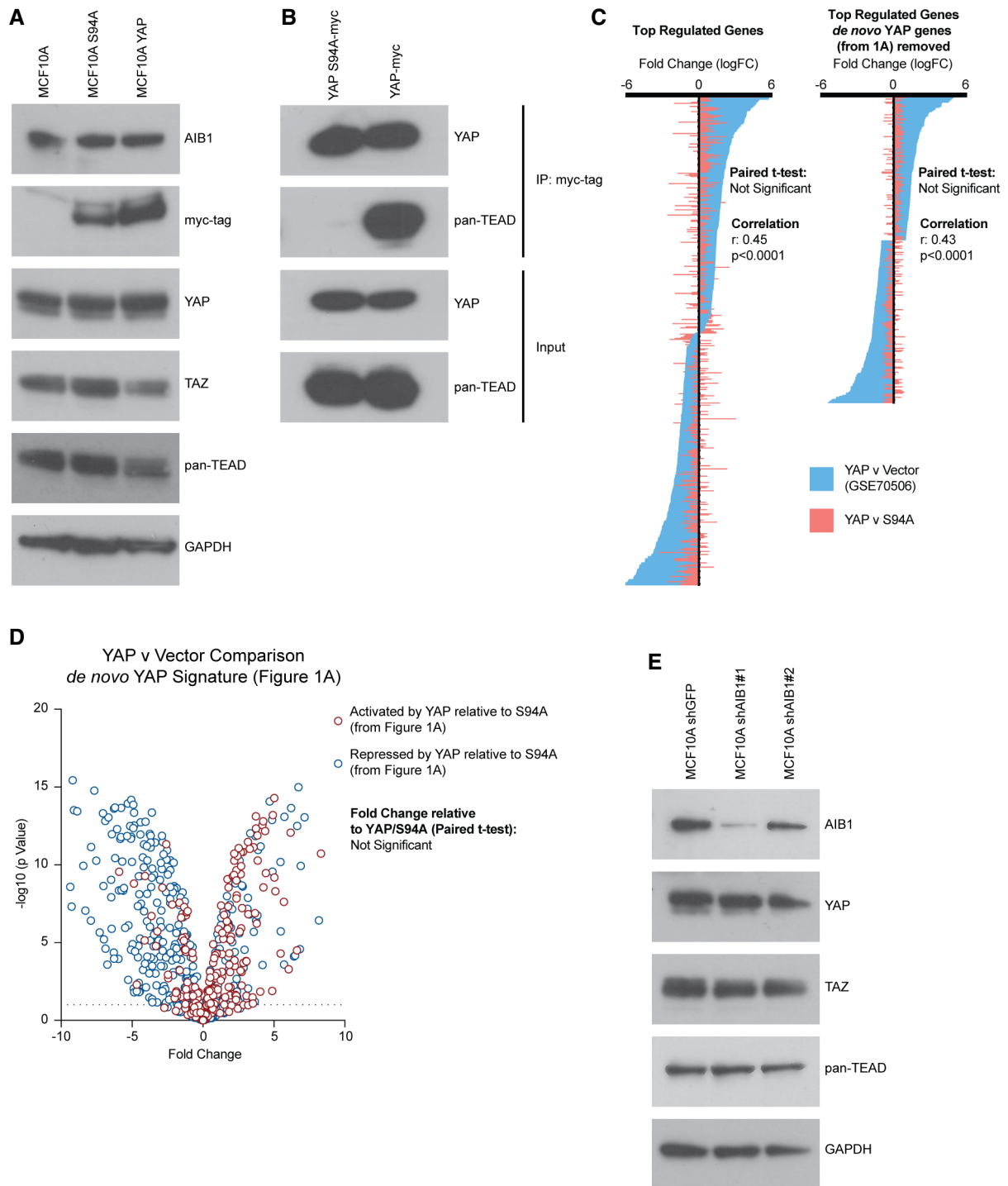


Figure EV2.

**Figure EV2. YAP S94A-expressing cells are similar to vector control.**

- A Overexpression of YAP or YAP S94A does not significantly alter the expression of endogenous AIB1, YAP, TAZ, or TEADs. Western blot analysis of indicated proteins following YAP S94A or YAP overexpression compared to parental baseline. Asterisk indicates non-specific band.
- B YAP S94A does not interact with TEAD. Co-immunoprecipitation of myc-tagged YAP S94A or YAP performed with myc antibody. Immunoblots show co-IP and input lysate; membranes were probed with antibodies as indicated.
- C Gene expression changes between YAP and YAP S94A are not significantly different from YAP relative to vector control (GSE70506) and are significantly correlated. Waterfall plot comparing significantly regulated genes ( $> 2$ FC an  $P < 0.05$ ), to significantly regulated genes following removal of *de novo* YAP signature genes (Fig 1) in MCF10A YAP vs. vector control to YAP vs. YAP S94A.
- D *De novo* YAP signature expression changes between YAP and vector control are not significantly different than YAP relative to YAP S94A. Volcano plot showing change of YAP-activated and YAP-repressed genes (described in Fig 1A and B) in YAP vs. vector control.
- E Knockdown of AIB1 does not affect stabilization of YAP, TAZ, or TEADs. Western blot analysis of indicated proteins following AIB1 knockdown.

Source data are available online for this figure.

**Figure EV3. ANCO1 knockdown in normal mammary epithelial and early-stage breast cancer cell lines.**

- A Positive control PLA, showing foci (white foci, falsely colored 594 nm signal) of interaction between YAP-TEAD and AIB1-ANCO1. Representative image; scale bars shown indicate 25  $\mu$ m.
- B Single antibody negative PLA controls showing baseline signal in MCF10A shGFP (control) cells. Scale bars shown indicate 25  $\mu$ m.
- C PLA foci are significantly reduced between ANCO1-TEAD, ANCO1-YAP, AIB1-TEAD, and AIB1-YAP following AIB1 knockdown. Quantification of proximity ligation assays shown in Fig 2A.
- D Levels of endogenous *ANCO1* in MCF10A cells following knockdown of ANCO1; levels were assessed by RT-qPCR.
- E Levels of AIB1, YAP, TAZ, and TEADs are unaffected by ANCO1 depletion. Immunoblot of MCF10A cells following knockdown of ANCO1.
- F Levels of endogenous *ANCO1* in MCFDCIS cells following infection of shANCO1; levels were assessed by RT-qPCR.
- G Immunoblot of MCFDCIS cells following knockdown of ANCO1.
- H Levels of ANCO1 are not changed by overexpression of YAP or YAP S94A. Immunoblot of ANCO1 in MCF10A cells following overexpression.
- I Levels of ANCO1 are not changed by AIB1 knockdown. Immunoblot of ANCO1 in MCF10A cells following AIB1 knockdown.
- J 1q21.3 genes are suppressed by YAP overexpression relative to vector control. Gene set enrichment analysis of RNA-seq in MCF10A cells overexpressing YAP or empty vector (GSE70506).
- K Genes regulated by YAP overexpression on the 1q21.3 locus. Volcano plot of 1q21.3 genes with indicated S100A and SPRR family genes from GSE70506.
- L YAP represses 1q21.3 localized genes. Levels of endogenous *S100* and *SPRR* genes in MCF10A cell lines following overexpression of YAP or vector control; levels were assessed by RT-qPCR.
- M Levels of endogenous TEAD targets in MCF10A and MCFDCIS cell lines following infection of shANCO1; levels were assessed by RT-qPCR.
- N ANCO1 is moderately enriched at *CTGF* and *CYR61* promoters; in contrast, AIB1, TEAD4, and YAP are robustly recruited to these promoters. Chromatin immunoprecipitation (ChIP) performed in MCF10A cells. Levels of precipitated chromatin assessed by qPCR.
- O TEAD is engaged at *S100A7* proximal enhancer region within 1q21.3. Analysis of TEAD4 ChIP-seq in MDA-MB-231(GSE66081), MCF7, and A549 Cells (GSE32465) at 1q21.3.
- P AIB1 and TEAD are detected at superenhancer sites in normal mammary cells that were identified in other cancer cell lines. Analysis of AIB1 and TEAD4 ChIP-seq peaks at 1q21.3 in MCF10A cells.

Data information: Student's *t*-test was used for the statistical analysis in panels (C, D, F, L, M, and N); data represent the means  $\pm$  SD from at least three biological replicates (\* $P < 0.05$ , \*\* $P < 0.01$ , \*\*\* $P < 0.001$ , \*\*\*\* $P < 0.0001$ , ns = not significant). GSEA enrichment score and FDR used in panel (J). RNA-sequencing statistics in panel (K) were calculated by EdgeR with Benjamini-Hochberg multiple test correction in R.

Source data are available online for this figure.

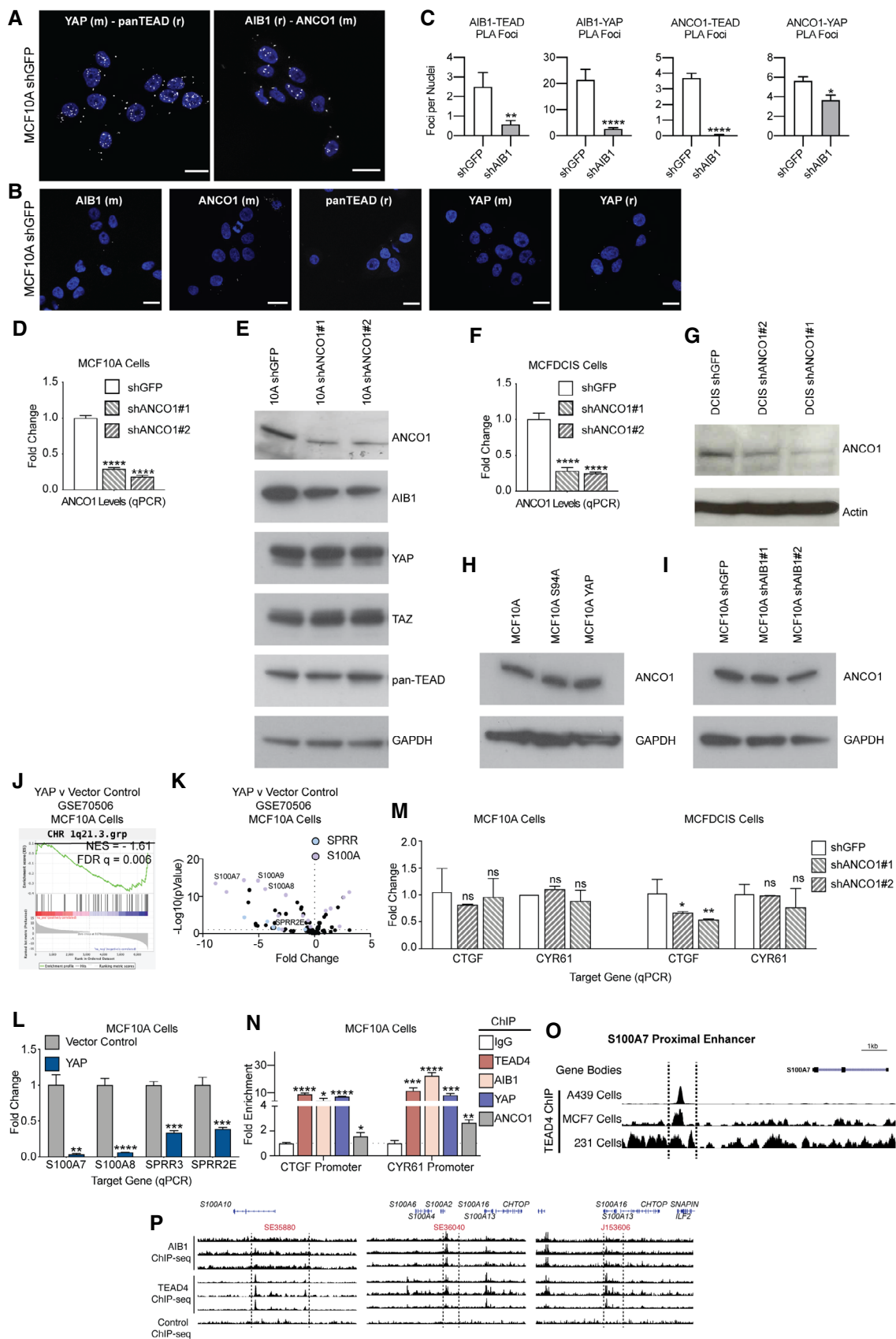
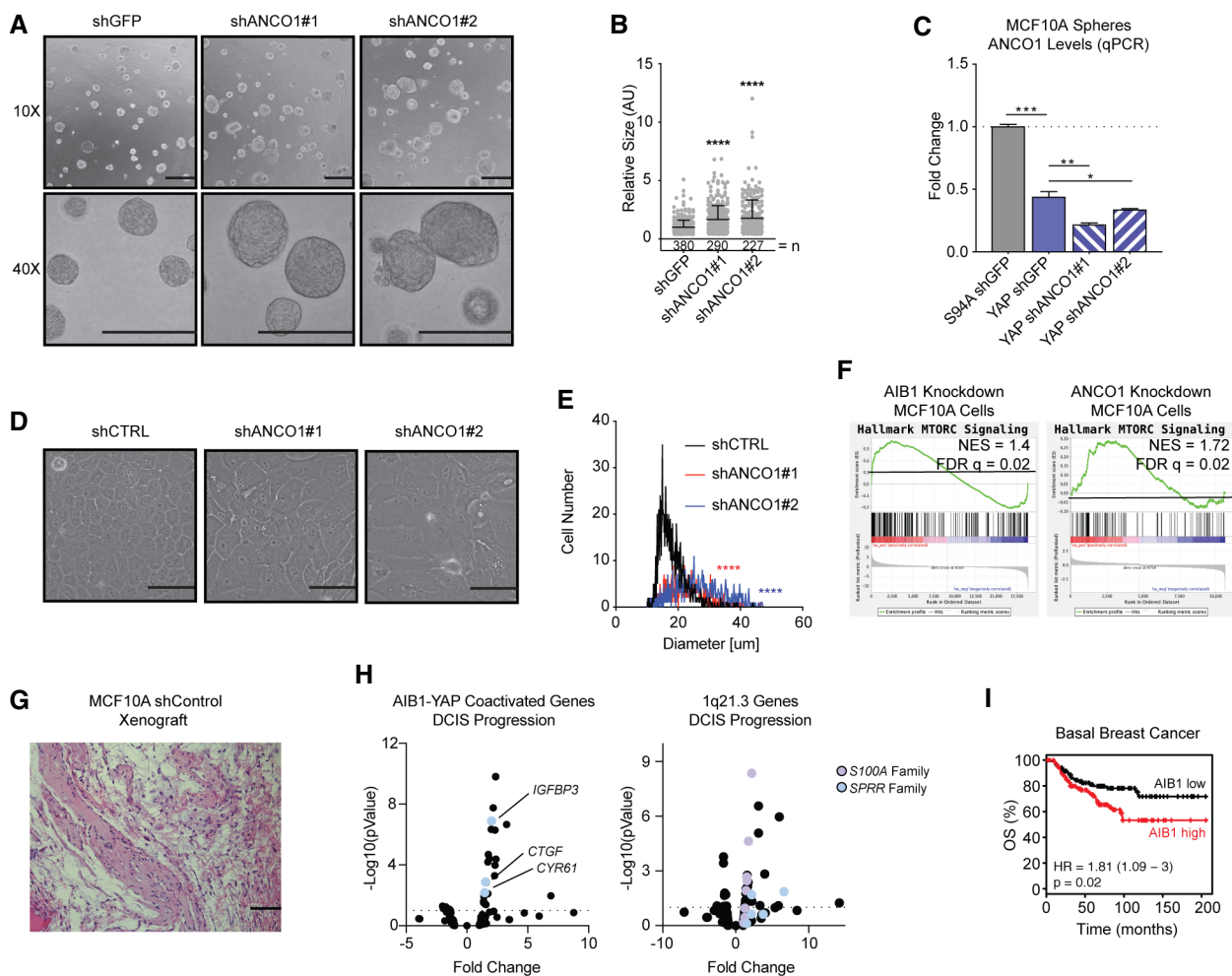


Figure EV3.



**Figure EV4. ANCO1 reduction results in larger single cells and spheres in 3D culture.**

- A ANCO1 knockdown increases the size of MCF10A spheres. Indicated cells were plated on Matrigel and allowed to form spheres for 7 days. 10 $\times$  and 40 $\times$  magnifications shown, scale bar = 100  $\mu$ m.
- B Quantification of size (arbitrary units) of aberrant spheres per field displayed in panel (A), relative to control 10A shGFP spheres.  $n$  = number of spheres.
- C ANCO1 levels decrease with YAP overexpression in spheres. ANCO1 mRNA levels were assessed by RT-qPCR.
- D ANCO1 loss increases cell size. Representative brightfield images of MCF10A cells with control shRNA or shANCO1. Scale bar = 100  $\mu$ m.
- E Quantification of cell size following ANCO1 knockdown in panel (C).
- F AIB1 and ANCO1 knockdown amplifies MTORC1 downstream genes. Gene set enrichment analysis of RNA-seq data and cDNA array data generated from MCF10A cell lines as indicated.
- G MCF10A cells are non-tumorigenic *in vivo*. Representative H&E staining of MCF10A xenograft in athymic nude mice at day 39 after cell implantation. Fibrotic, benign lesions shown, 20 $\times$  magnification; scale bar = 100  $\mu$ m.
- H AIB1-YAP co-activated genes and genes at the 1q21.3 locus increase during DCIS progression. Volcano plot of RNA-seq data from MCFDCIS xenografts during invasive progression. Select upregulated genes indicated.
- I High AIB1 levels are a poor prognostic indicator in basal breast cancer in patients. KM plot showing overall survival in patients with stratified ANCO1 expression.  $n$  = 360 patients.

Data information: Number of spheres quantified in panel (B) described above, with middle lines and error bars indicating mean  $\pm$  SEM. Kruskal-Wallis with Dunn's multiple comparison (non-parametric test used because data were non-normally distributed) in panel (B). Student's  $t$ -test was used for the statistical analysis in panels (C and E); data represent the means  $\pm$  SD from at least three replicates. GSEA enrichment score and FDR used in panel (F). RNA-sequencing statistics in panel (H) were calculated by EdgeR with Benjamini-Hochberg multiple test correction in R. KMPlot statistics were calculated by KMplotter in panel (I). \* $P$  < 0.05, \*\* $P$  < 0.01, \*\*\* $P$  < 0.001, \*\*\*\* $P$  < 0.0001.

Source data are available online for this figure.